



## Technical Note

# Synthesis, structural studies and antioxidant activities of M(II) complexes with NOS donor schiff base ligand

Nevin TURAN<sup>1,\*</sup>, Mustafa BİNGÖL<sup>2</sup>, Ahmet SAVCI<sup>3</sup>, Enver Fehim KOÇPINAR<sup>4</sup>,  
Naki ÇOLAK<sup>5</sup>

<sup>1</sup>Muş Alparslan University, Faculty of Arts and Sciences, Department of Chemistry, Muş, Turkey

<sup>2</sup>Muş Alparslan University, Faculty of Arts and Sciences, Department of Chemistry, Muş, Turkey

<sup>3</sup>Muş Alparslan University, Faculty of Arts and Sciences, Department of Molecular Biology and Genetics, Muş, Turkey

<sup>4</sup>Muş Alparslan University, Vocational School, Department of Medical Services and Techniques, Muş, Turkey

<sup>5</sup>Hitit University, Department of Chemistry, Faculty of Arts and Sciences, Çorum, Turkey

## ARTICLE INFO

### Article history

Received: 23 September 2020

Accepted: 21 January 2021

### Key words:

Biological activity; Transition metal complexes; NOS donor schiff base; Spectral properties

## ABSTRACT

Schiff base ligand, (*E*)-methyl 6-acetamido-2-(5-bromo-2-hydroxybenzylideneamino)-4,5,6,7-tetrahydrobenzo[*b*]thiophene-3-carboxylate, was successfully prepared with condensation reaction. The newly obtained Schiff base used to synthesize five new complex, [FeLCl(H<sub>2</sub>O)<sub>2</sub>].1.5H<sub>2</sub>O, [CoLCl(H<sub>2</sub>O)<sub>2</sub>].2H<sub>2</sub>O, [NiLCl(H<sub>2</sub>O)<sub>2</sub>].H<sub>2</sub>O, [RuLCl(*p*-cymene)].3.5H<sub>2</sub>O and [PdLCl.H<sub>2</sub>O].3H<sub>2</sub>O. From the magnetic and spectral data, the geometric structures of these complexes were found to be square planar and octahedral. The characterizations of ligand and complexes were done by FT-IR, UV-Vis, <sup>1</sup>H and <sup>13</sup>C-NMR, microanalyses, magnetic susceptibility, mass spectra and thermogravimetry analysis (TGA) and further were screened for antioxidant activities. Antioxidant properties of synthesized compounds were examined using different methods including total antioxidant activity, FRAP (ferric reducing antioxidant power), CUPRAC (cupric reducing antioxidant capacity) and DPPH (2,2-diphenyl-1-picrylhydrazyl). The Ru(II), Pd(II), Fe(II) and Co(II) metal complexes generally exhibited good antioxidant properties.

**Cite this article as:** Turan N, Bingöl M, Savci A, Koçpinar EF, Çolak N. Synthesis, structural studies and antioxidant activities of m(ii) complexes with NOS donor schiff base ligand. Sigma J Eng Nat Sci 2021;39(3):279–289.

## INTRODUCTION

In recent years, Schiff base metal complexes have taken wide attention due to broad applications such as anticancer, antioxidant, antifungal and anticonvulsant-centigrade,

corrosion inhibition and also anti-inflammatory activity [1–3]. The azomethine functional group (C=N) has extraordinary donor properties and is vital for coordination chemistry. The Schiff bases-complexes derived from substituted

\*Corresponding author.

\*E-mail address: nevintrn@hotmail.com

This paper was recommended for publication in revised form by Regional Editor Emel Akyol



salicylaldehydes and various aromatic amines are widely researched and represent an important class of coordination chemistry with unusual configuration, structural variability, and sensitivity to molecular environments [4]. The Schiff base complexes derived from salicylaldehyde and its derivatives with primary amines that contain the  $N_2O$ ,  $N_2S$ ,  $NO_2$ , or  $NOS$  donor sets, have interesting biological activities [5].

Our research group is interested in synthesis, characterization and the biological activities of new Schiff base ligands and complexes [6–9]. In the present study, the new Schiff base and its metal complexes were synthesized because of their chemical and biological properties. Furthermore, antioxidant activity of all the synthesized compounds was investigated. The results showed that antioxidant properties of complexes generally were better than ligand. No studies on the antioxidant properties of the Schiff base and metal complexes that we synthesized have been found in the literature.

## EXPERIMENTAL

### Reagents and Instrumentation

All solvents and chemicals were purchased from the Sigma chemical company and were utilized with no further any purified. FT-IR data were obtained from KBr pellets in the range of 4000 to 400  $cm^{-1}$  on a Perkin Elmer 65 spectrometer. The  $^1H$  and  $^{13}C$ -NMR spectra were recorded on Bruker Avance 300 (300 MHz), the chemical shifts ( $\delta$ ) were expressed in ppm down field from TMS as internal reference. The UV-Vis spectra were recorded on a Shimadzu 1800 spectrophotometer. Mass spectra were performed using an AGILENT 1100 MSD spectrophotometer. The elements N, H, C and S were analyzed with the PerkinElmer 240C analyzer. The magnetic susceptibility measured at room temperature, a Gouy balance using  $Hg[Co(SCN)_4]$  as the calibrant. The thermal gravimetric analysis (TGA) was made from room temperature up to 800  $^{\circ}C$  at a heating range of 10  $^{\circ}C/min$  using nitrogen atmosphere.

### Synthesis and Characterization of Schiff Base Ligand (L)h

0.60 g (3 mmol) 5-bromo-2-hydroxybenzaldehyde and 1.35 g (3 mmol) of starting material, methyl 6-acetamido-2-amino-4,5,6,7-tetrahydrobenzo[*b*]thiophene-3-carboxylate, were mixed in ethanol (20 mL). The reaction mixture was boiled for 4 h under reflux. Light orange ligand obtained was

filtered through filter paper, washed with ethanol, and dried over fused calcium chloride. Synthesis scheme of the Schiff base ligand was given in Figure 1.

The ligand (L) was attained as a light orange solid with 85% yield. m.p.: 243–246  $^{\circ}C$ . Molecular weight: 451.33 g/mol. Elemental analysis Calc. for (%)  $C_{19}H_{19}BrN_2O_4S$ : C, 50.51; H, 4.20; N, 6.20; S, 7.09; Found: C, 50.60; H, 4.18; N, 6.20; S, 7.10. IR ( $\nu$ ,  $cm^{-1}$ ): 3434, 3290, 3180, 3060, 2944, 1707, 1638, 1562, 1545, 1484, 1251, 730.  $^1H$ -NMR (DMSO- $d_6$ ,  $\delta$ , ppm): 11.26 (s, 1H, -OH), 8.77 (s, H, CH = N), 8.14 (d, H, -NH), 7.80–6.81 (m, 3H, Ar-CH), 3.89 (s, 3H, -OCH<sub>3</sub>), 3.95–1.72 (m, 7H, cyclohexyl), 1.84 (s, 3H, -CH<sub>3</sub>).  $^{13}C$ -NMR (DMSO- $d_6$ ,  $\delta$ , ppm): 170.10, 159.90 (2C = O), 160.00 (CH = N), 150.70–128.60 (thionyl ring), 53.00–18.30 (cyclohexyl), 51.50 (-OCH<sub>3</sub>), 23.60 (-CH<sub>3</sub>). UV-Vis ( $\lambda_{max}$ , nm):  $\pi \rightarrow \pi^*$ , 206 (70), 215 (129), 225 (537), 235 (210), 258 (1093);  $n \rightarrow \pi^*$ , 290 (58), 400 (94).

### Synthesis and Characterization of Complexes

20 mL ethanol solution of 1.00 g (2 mmol) Schiff base ligand and 10 mL ethanol solution of 0.40 g (2 mmol) of  $FeCl_2 \cdot 4H_2O$  were mixed and refluxed for 8 hours with a magnetic stirrer. A dark green precipitate was filtered, washed with ethanol and air dried. Similar synthesis method was performed in other complex compounds using 0.47 g (2 mmol)  $CoCl_2 \cdot 6H_2O$ , 0.47 g (2 mmol)  $NiCl_2 \cdot 6H_2O$ , 0.70 g (1 mmol)  $[RuCl_2(p\text{-cymene})_2]$ , 0.56 g (2 mmol)  $PdCl_2(CH_3CN)_2$  metal salts. The suggested structures for the complexes were shown in Figure 2.

$[FeLCl(H_2O)_2] \cdot 1.5H_2O$ : Yield: 80%. Color: Black. m.p.: > 250  $^{\circ}C$ . Molecular weight: 604.22 g/mol.  $\mu_{eff}$  (B.M.): 4.90. Elemental analysis Calc. for (%)  $(C_{19}H_{25}N_2O_{7.5}BrSFeCl)$ : C, 37.73; H, 4.13; N, 4.63; S, 5.29; Found: C, 38.00; H, 4.25; N, 4.58; S, 5.34. IR (KBr,  $\nu$   $cm^{-1}$ ): 3426, 3296, 3100, 3047, 2975, 2933, 1706, 1630, 1592, 1569, 1478, 1274, 722, 597, 523, 499, 457. UV-Vis ( $\lambda_{max}$ , nm):  $\pi \rightarrow \pi^*$ , 217 (2112), 222 (2002), 231 (1923), 239 (949);  $n \rightarrow \pi^*$ , 293 (525), 404 (741), 526 (38), 562 (27), 573 (26), 745 (11), 968 (6). ESI-MS:  $m/z$  570.22 (Calc.), 570.37 (Found)  $[M+2H-2H_2O]^{2+}$ .

$[CoLCl(H_2O)_2] \cdot 2H_2O$ : Yield: 75%. Color: Brown. m.p.: > 250  $^{\circ}C$ . Molecular weight: 616.33 g/mol.  $\mu_{eff}$  (B.M.): 4.70. Elemental analysis Calc. for (%)  $(C_{19}H_{26}N_2O_8BrSCoCl)$ : C, 37.00; H, 4.21; N, 4.54; S, 5.19; Found: C, 37.10; H, 4.42; N, 4.60; S, 5.17. IR (KBr,  $\nu$   $cm^{-1}$ ): 3525, 3428, 3119, 2986, 2937, 1706, 1647, 1598, 1593, 1477, 1279, 722, 594, 573, 540, 473. UV-Vis ( $\lambda_{max}$ , nm):  $\pi \rightarrow \pi^*$ , 218 (2467), 224 (1144), 237

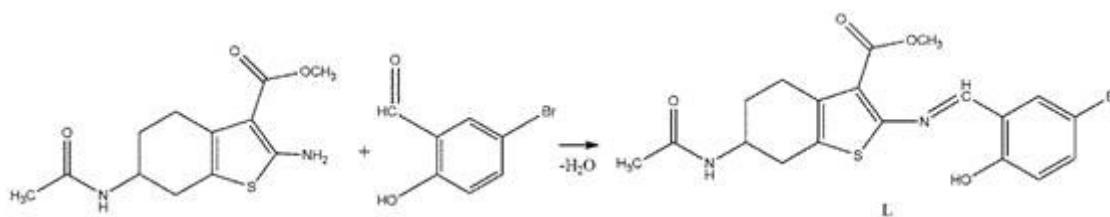


Figure 1. Synthesis scheme of Schiff base ligand.

(1048), 242 (2937), 262 (3703);  $n \rightarrow \pi^*$ , 410 (2105), 596 (85), 608 (86), 670 (93). ESI-MS:  $m/z$  614.33 (Calc.), 614.57 (Found)  $[M-2H]^{2+}$ .

$[\text{NiLCl}(\text{H}_2\text{O})_2] \cdot \text{H}_2\text{O}$ : Yield: 76%. Color: Orange. m.p.:  $> 250$  °C. Molecular weight: 598.49 g/mol.  $\mu_{\text{eff}}$  (B.M.): 3.87. Elemental analysis Calc. for (%) ( $\text{C}_{19}\text{H}_{24}\text{N}_2\text{O}_7\text{BrSNiCl}$ ): C, 38.09; H, 4.01; N, 4.67; S, 5.34; Found: C, 37.90; H, 4.00; N, 4.62; S, 5.32. IR (KBr,  $\nu$   $\text{cm}^{-1}$ ): 3423, 3335, 3120, 2979, 2948, 1706, 1645, 1596, 1577, 1477, 1278, 720, 556, 523, 491, 459. UV-Vis ( $\lambda_{\text{max}}$ , nm):  $\pi \rightarrow \pi^*$ , 215 (186), 223 (644), 238 (871), 245 (291), 251 (2275), 271 (463);  $n \rightarrow \pi^*$ , 373 (262), 385 (266), 500 (343). ESI-MS:  $m/z$  570.49 (Calc.), 570.38 (Found)  $[M-H-1.5\text{H}_2\text{O}]^+$ .

$[\text{PdLCl}(\text{H}_2\text{O})] \cdot 3\text{H}_2\text{O}$ : Yield: 60%. Color: Brown. m.p.:  $> 250$  °C. Molecular weight: 663.49 g/mol.  $\mu_{\text{eff}}$  (B.M.): Dia. Elemental analysis Calc. for (%) ( $\text{C}_{19}\text{H}_{26}\text{N}_2\text{O}_8\text{BrSPdCl}$ ): C, 34.36; H, 3.92; N, 4.22; S, 4.82; Found: C, 34.40; H, 3.82; N, 4.20; S, 4.95. IR (KBr,  $\nu$   $\text{cm}^{-1}$ ): 3434, 3373, 3203, 3070, 2967, 2937, 1706, 1651, 1579, 1556, 1475, 1236, 730, 584, 559, 505, 467. UV-Vis ( $\lambda_{\text{max}}$ , nm):  $\pi \rightarrow \pi^*$ , 217 (1155), 224 (323), 230 (422), 237 (431);  $n \rightarrow \pi^*$ , 303 (273), 577 (53). ESI-MS:  $m/z$  664.49 (Calc.), 664.58 (Found)  $[M+H]^+$ .

$[\text{RuLCl}(p\text{-cymene})] \cdot 3.5\text{H}_2\text{O}$ : Yield: 66%. Color: Black. m.p.:  $> 250$  °C. Molecular weight: 779.37 g/mol.  $\mu_{\text{eff}}$  (B.M.): Dia. Elemental analysis Calc. for (%) ( $\text{C}_{29}\text{H}_{35}\text{N}_2\text{O}_{7.5}\text{BrSRuCl}$ ): C, 44.65; H, 4.49; N, 3.59; S, 4.10; Found: C, 44.60; H, 4.70; N, 3.52; S, 4.15. IR (KBr,  $\nu$   $\text{cm}^{-1}$ ): 3434, 3305, 3070, 2956, 2918, 1705, 1655, 1560, 1456, 1259, 729, 522, 482, 461. UV-Vis ( $\lambda_{\text{max}}$ , nm):  $\pi \rightarrow \pi^*$ , 220 (687), 224 (174), 234 (1683), 242 (1268), 252 (3238), 260 (2114);  $n \rightarrow \pi^*$ , 404 (768), 611 (23), 669 (23). ESI-MS:  $m/z$  778.37 (Calc.), 778.65 (Found)  $[M-H]^+$ .

## Antioxidant Assays

The antioxidant properties of synthesized compounds were determined by total antioxidant activity, FRAP, CUPRAC, DPPH free radical scavenging methods. The applied methods were performed as described previously in the literature [10].

## RESULT AND DISCUSSION

### Spectroscopic Studies

When IR spectra of Schiff base ligand was examined, unlike the starting material, the seeing of a new band belong to azomethine group ( $\text{CH} = \text{N}$ ) at  $1638$   $\text{cm}^{-1}$  [11], observation of OH stretching vibration  $3434$   $\text{cm}^{-1}$  and observation of C-Br stretching vibration at  $1028$ – $1025$   $\text{cm}^{-1}$  indicated that Schiff base synthesis occurred [12]. The carbonyl stretch in all synthesized compounds was presented above  $1700$   $\text{cm}^{-1}$ , while the NH stretching vibration was presented at over  $3200$   $\text{cm}^{-1}$  as a broad signal. The azomethine band in  $1638$  in ligand showed shifts slightly to lower or higher energy in all complexes. The shifts to a low or high frequency in the spectrum of complexes at  $1630$ ,  $1647$ ,  $1645$ ,  $1651$  and  $1655$   $\text{cm}^{-1}$  for Co(II), Ni(II), Fe(II), Pd(II) and Ru(II), respectively, were owing to participation of the N atom of the  $\text{CH} = \text{N}$  group in coordination. The IR spectra of metal complexes indicated that the phenolic OH band disappeared, there was an increasing in  $\nu(\text{C-O})$  at  $1236$ – $1274$   $\text{cm}^{-1}$ , the indicative of deprotonation and M-O bond were formed. Some new bands in the FT-IR spectrum of complexes in the regions  $594$ – $522$  and  $505$ – $457$   $\text{cm}^{-1}$  were likely owing to M-O and M-N bands, respectively [13]. In addition,  $\nu(\text{C-S-C})$  band seen in the region  $730$   $\text{cm}^{-1}$  in the

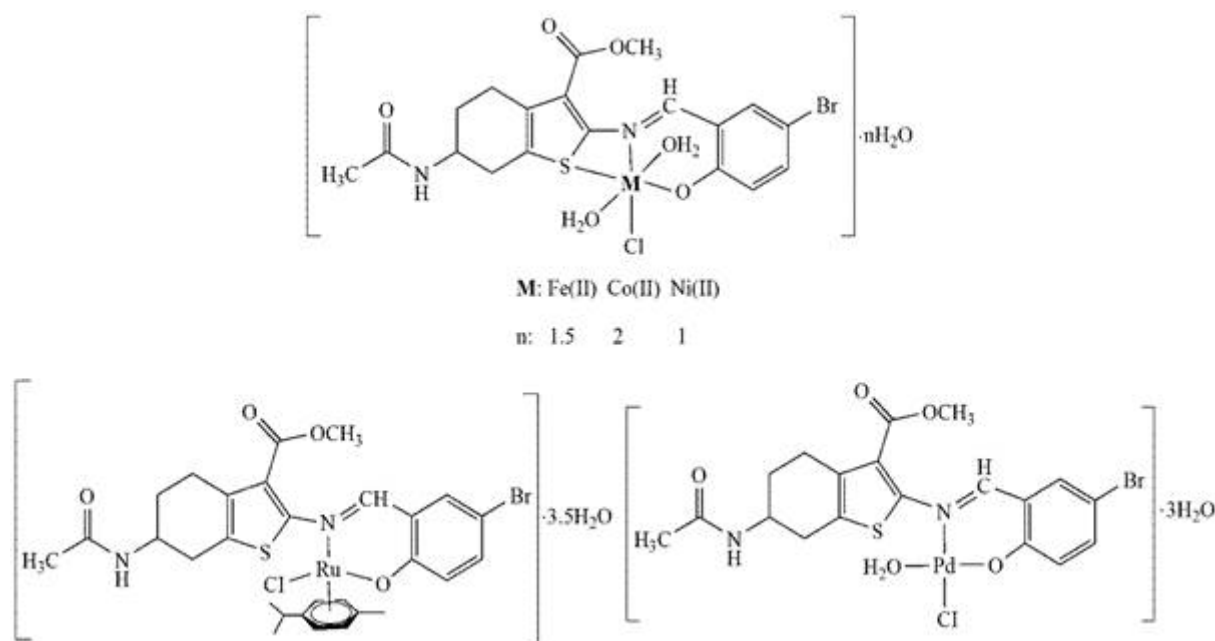


Figure 2. Structure of complexes.

ligand remained unchanged on complexation of the Ru(II) and Pd(II). The ligand C-Br band at  $1025\text{ cm}^{-1}$  was not changed at complexes. This showed that C-Br group didn't take part in coordination.

When the  $^1\text{H-NMR}$  spectra of Schiff base was examined, the most important peak was the peak of azomethine proton. The proton bound to the azomethine group was usually resonance in the range of  $\delta = 8\text{--}9$  ppm. When the  $^1\text{H-NMR}$  spectra obtained by dissolving the synthesized Schiff base compound in  $\text{DMSO-d}_6$ , the peak of azomethine hydrogen was observed as 8.77 ppm and OH proton singlet as 11.26 ppm as expected. The peak of azomethine carbon was seen in the  $^{13}\text{C-NMR}$  spectrum at 160.00 ppm. It was observed that the obtained NMR results supported the formation of the compound and were consistent with the literature [14]. Further evidence for the presence of coordinated Schiff base ligand in the new complexes was provided by the  $^1\text{H}$  NMR spectra of the complexes. In the Ru(II) and Pd(II) complexes the signals due to the azomethine proton ( $\text{CH} = \text{N}$ ) appeared as a singlet at 7.56 and 7.76 ppm, respectively. Signals appeared in the 6.55–7.42 ppm region for Ru(II) and 6.77–11.38 ppm for Pd(II) was assigned to the phenyl ring and pyridine protons. Also in the complexes Ru(II) and Pd(II)  $\text{NH}_2$  protons appeared between 7.90 and 8.37 ppm and 8.01–9.92 ppm, respectively.

The UV-vis spectra of ligand and its metal complexes were recorded in ethanol from 200 to 800 nm at room temperature. The bands between 206 and 258 nm were able to assign to  $\pi \rightarrow \pi^*$  transitions of the phenyl and thiophene rings. The electronic spectra of ligand showed bands at 290 and 400 nm which attributed to  $n \rightarrow \pi^*$  and these bands disappeared upon chelation [15,16]. In the UV-vis spectra of the Fe(II), Co(II), Ni(II), Ru(II) and Pd(II) complexes, peaks in the range of 217–293, 218–262, 215–271, 217–303 and 217–303 nm showed transitions  $\pi \rightarrow \pi^*$  and  $n \rightarrow \pi^*$ , respectively. The magnetic susceptibility value of the Fe(II) complex was measured as 4.90 B.M. [17]. The peak observed in the mass spectrum of the compound,  $m/z$ : 570.37, corresponded to  $[\text{M}+2\text{H}-2\text{H}_2\text{O}]^{2+}$ . In the UV-vis spectra of the Co(II) complex, the absorption bands at 410, 596 and 608 nm were caused by ligand to metal charge transfer. The peak observed in the mass spectrum of the compound,  $m/z$ : 614.57, corresponded to  $[\text{M}-2\text{H}]^{2+}$ . The susceptibility value of Co(II) complex was measured as 4.70 B.M. This observed value supported the formation of octahedral structure [18]. In the UV-vis spectrum of the Ni(II) complex, the bands at 373, 385 and 500 nm indicated load transfer transitions. The magnetic susceptibility value of the Ni(II) complex was 3.87 B.M. This observed value supported the formation of the octahedral structure. The peak observed in the mass spectrum of the compound,  $m/z$ : 570.38, corresponded to  $[\text{M}-\text{H}-1.5\text{H}_2\text{O}]^+$ . The band at 577 nm in the UV-vis spectra of the Pd(II) complex showed the charge transfer transition (MLCT) from the metal to the ligand [19]. The peak observed in the mass spectra of the compound,  $m/z$ :

664.58, corresponded to  $[\text{M}+\text{H}]^+$ . The all characterization results given in the material and method section showed that Pd(II) had square planar structure [20].

It was suggested that Fe(II), Co(II), Ni(II) and Ru(II) complexes had octahedral structure and Pd(II) had square planar structure from magnetic susceptibility, elemental analysis and UV-vis spectrum results. Fe(II), Co(II) and Ni(II) complexes were seen to be paramagnetic and Ru(II) and Pd(II) complexes were diamagnetic.

All complexes were formed only in the powder form, which was not suitable for single X-ray diffraction analysis. Attempts to isolate single crystal suitable for X-ray diffraction measurement were not successful. However, structures of these complexes were proposed based upon the analytical, spectroscopic, thermal and magnetic data.

### Thermal Studies

At first step of the thermal analysis diagram of Fe(II) complex, 3.5 moles of hydrate and coordinated waters, Cl and  $\text{OCH}_3$  groups were removed (calc. 21.43%) with mass loss of 21.00% in the temperature range of 50–230 °C. At the second step, it was seen that  $\text{C}_3\text{H}_4\text{O}_2\text{N}$  group was removed with a mass loss of 14.50% in the range of 230–415 °C (calc. 14.90%). At the range of 415–700 °C, it was observed that the decomposition continued with the losing of  $\text{C}_{14}\text{H}_{11}\text{Br}$  group.

When the thermal analysis results of Co(II) complex were examined, in the first step it was seen that 2 moles of hydrate water molecule were removed from the structure with a mass loss of 5.20% (calc. 5.84%) between 50–100 °C. At the second step, 2 moles of coordinated water and Cl atom were removed from the structure with mass loss of 11.20% (calc. 11.59%) in the temperature range of 100–210 °C. At the third step,  $\text{C}_2\text{H}_3\text{O}_2$  group was removed from the structure with mass loss of 9.80% (calc. 9.57%) between 210–270 °C. In the fourth step at range of 270–410 °C and in the fifth step at the range of 410–650 °C, the remaining compound decayed and CoO remained as waste with 13.71% [21]. Similar degradations were observed in other complexes and the results obtained were given in Table 1.

### DPPH Free Radical Scavenging Activity

The basis of the method is the reduction of the DPPH radical by mixing the solution containing DPPH and the solution of a molecule (antioxidant) which has a tendency to give hydrogen atom and the loss of the initially purple color of the solution. The reaction is followed by measuring the decrease in absorbance of the purple-colored solution around 517 nm [22,23].

DPPH radical scavenging activity of ligand and complexes decreased with the increases in sample concentrations. DPPH radical scavenging activity at a concentration of 100  $\mu\text{g/mL}$  of standards, ligand and complexes are as follows: TRLX (92.87%) > BHA (79.73%) > Ru(II) (45.58%) > Fe(II) (29.47%) > Co(II) (29.21%) > Pd(II) (26.93%) > Ni(II) (8.85%) > L (2.58%).

**Table 1.** Thermogravimetric analysis data for the synthesized M(II) complexes

Compounds	Decomposition step	Temp. range, °C	Weight loss, %		Decomposition product
			Calc.	Found	
[FeLCl(H <sub>2</sub> O) <sub>2</sub> ].1.5H <sub>2</sub> O	1 <sup>st</sup>	50–230	21.43	21.00	3.5H <sub>2</sub> O, Cl, OCH <sub>3</sub>
	2 <sup>nd</sup>	230–415	14.90	14.50	C <sub>3</sub> H <sub>4</sub> O <sub>2</sub> N
	3 <sup>rd</sup>	415–700	42.52	42.20	C <sub>14</sub> H <sub>11</sub> Br
	Residue		21.15		
[CoLCl(H <sub>2</sub> O) <sub>2</sub> ].2H <sub>2</sub> O	1 <sup>st</sup>	50–100	5.84	5.20	2H <sub>2</sub> O
	2 <sup>nd</sup>	100–210	11.59	11.20	2H <sub>2</sub> O, Cl
	3 <sup>rd</sup>	210–270	9.57	9.80	C <sub>2</sub> H <sub>3</sub> O <sub>2</sub>
	4 <sup>th</sup>	270–410	16.80	16.00	C <sub>6</sub> H <sub>11</sub> ON
	5 <sup>th</sup>	410–650	42.49	42.00	C <sub>11</sub> H <sub>4</sub> BrSN
	Residue		13.71		CoO
[NiLCl(H <sub>2</sub> O) <sub>2</sub> ].H <sub>2</sub> O	1 <sup>st</sup>	50–130	3.00	2.80	H <sub>2</sub> O
	2 <sup>nd</sup>	130–210	17.11	16.80	2H <sub>2</sub> O, Cl, OCH <sub>3</sub>
	3 <sup>rd</sup>	210–305	14.36	14.00	C <sub>3</sub> H <sub>4</sub> O <sub>2</sub> N
	4 <sup>th</sup>	305–430	15.20	15.40	C <sub>7</sub> H <sub>7</sub>
	5 <sup>th</sup>	430–660	30.39	30.80	C <sub>7</sub> H <sub>4</sub> NBr
	Residue		19.94		
[RuLCl( <i>p</i> -cymene)].3.5H <sub>2</sub> O	1 <sup>st</sup>	50–220	25.27	25.20	3.5H <sub>2</sub> O, <i>p</i> -cymene ring (C <sub>10</sub> H <sub>14</sub> )
	2 <sup>nd</sup>	220–390	35.37	35.00	Cl, C <sub>10</sub> H <sub>14</sub> O <sub>3</sub> NBr
	3 <sup>rd</sup>	390–630	18.34	18.20	C <sub>9</sub> H <sub>4</sub> S
	Residue		21.00		
[PdLClH <sub>2</sub> O].3H <sub>2</sub> O	1 <sup>st</sup>	50–170	8.13	8.00	3H <sub>2</sub> O
	2 <sup>nd</sup>	170–385	73.42	72.00	Cl, C <sub>19</sub> H <sub>19</sub> O <sub>3</sub> N <sub>2</sub> SBr
	3 <sup>rd</sup>	385–770	18.45	17.60	PdO

The inhibition of free radicals by DPPH (%) was calculated as follows:

$$\text{DPPH radical scavenging activity \%} = [1 - A_1/A_0] \times 100$$

(The absorbance of A<sub>0</sub> control was taken as the absorbance of A<sub>1</sub> samples)

When DPPH free radical scavenging activity results were evaluated it was seen that Ru(II) (45.58%) complex had the highest effect compared to BHA (79.73%) and TRLX (92.87%) standards and ligand (2.58%) had the lowest effect in scavenging free radicals (Figure 3). Although the DPPH radical scavenging activity of the ligand was quite low, it can be said that the radical scavenging effects improved when it was made in a metal complex; however, it was also observed that the radical scavenging effects did not reach the effects of

standards. This result proves that the biological activity of the ligand can be improved by metals.

#### Reduction Power of Fe<sup>3+</sup> to Fe<sup>2+</sup> According to FRAP Method

In this method, in the presence of reducing agents such as an antioxidant, the Fe<sup>3+</sup>/ferricyanide complex is reduced to the ferrous form of the Fe<sup>2+</sup>/ferric cyanide complex. This complex forms a blue colored complex with adding FeCl<sub>3</sub> and gives maximum absorbance at 700 nm. The reduction capacities generally increase depending on the amount and absorbance of the samples [24]. The reduction power was found by measuring the absorbance at 700 nm and different concentrations (Figure 4).

In Figure 4, the reduction power capacities of the ligand and complexes were compared to the standard antioxidants

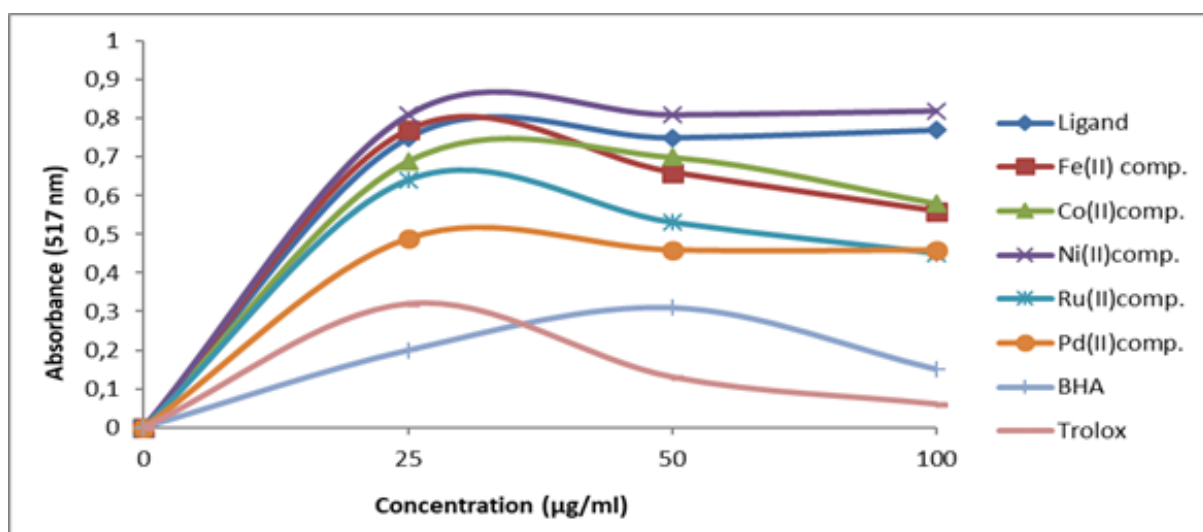


Figure 3. DPPH radical scavenging activities of ligand, metal complexes and standard antioxidants at 25, 50 and 100 µg/mL.

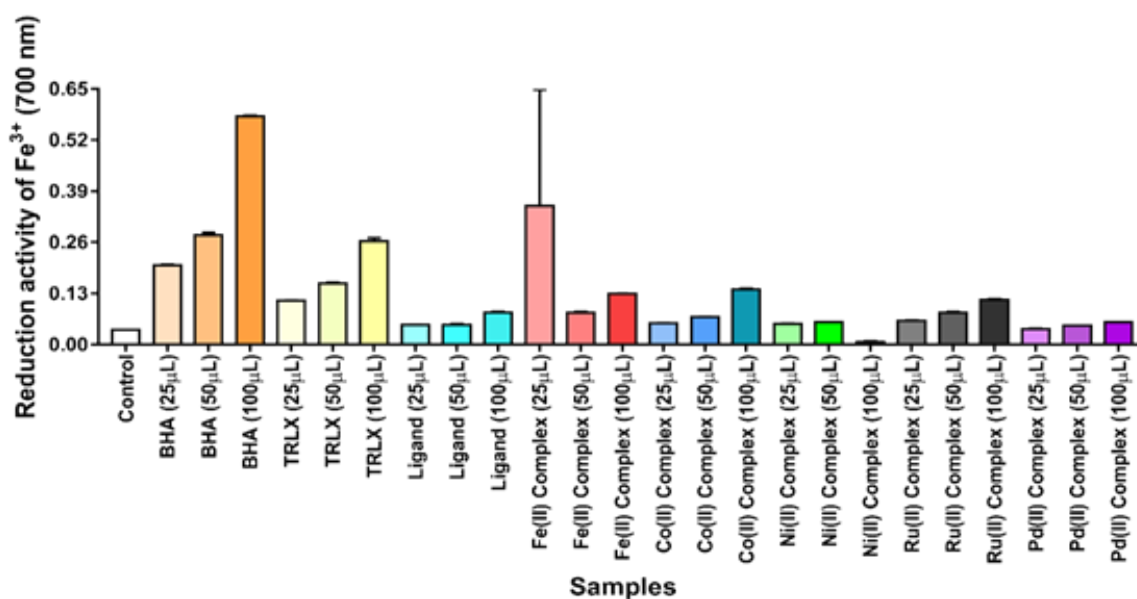


Figure 4. Ferric ions ( $\text{Fe}^{3+}$ ) reduction activities of standard antioxidants, ligand and its M(II) complexes using FRAP method.

for 100 µg/mL concentration and the results are as follows: BHA > TRLX > Co(II) > Fe(II) > Ru(II) > L > Pd(II) > Ni(II). FRAP results exhibited that Co(II) complex had the best capability compared to BHA. Although the iron reduction capacity of the ligand was far from the capacity of the standards, it was seen that the metal complexes with the closest iron reduction capacity to the standards were Ru(II) and Pd(II) complexes. Here, too, the radical scavenging effects of ligands became stronger with metals, as seen in DPPH radical scavenging activity results.

#### Reduction Power of Cupric Ions ( $\text{Cu}^{2+}$ ) to Cuprous Ions ( $\text{Cu}^+$ ) According to CUPRAC Method

Generally, the capacity of the ligand and its complexes to reduce cupric ions to ( $\text{Cu}^{2+}$ ) increases in direct proportional to the amount and absorbance of the samples. The complex formed by the cupric ions ( $\text{Cu}^{2+}$ ) with neocuprin is reduced to the cuprous ions ( $\text{Cu}^+$ ) in the presence of antioxidant agents. The light blue color of the media changes to yellow. The reduction capacity of solutions of the samples at different concentrations (25, 50 and 100 µg/mL) was

found by measuring their absorbance at maximum 450 nm [25,26] (Figure 5).

In Figure 5, reducing power capacities of the standards, the ligand and its complexes at concentration of 100 µg/mL are as follows: BHA > TRLX = Ru(II) > Co(II) > Pd(II) > Ni(II) > Fe(II) > L.

According to the CUPRAC method, when the reduction power results of cupric ions ( $\text{Cu}^{2+}$ ) to cuprous ions ( $\text{Cu}^+$ ) were examined, it was observed that ligand and complexes, standards and Ru(II) complex showed the best reduction power capacity according to increasing absorbances. In general, it can be said that the copper reduction capacity of the ligand and its complexes is better than the DPPH radical scavenging and iron reduction capacities. In addition to this, Ru(II) complex was detected to have similar effect to TRLX in the all concentrations.

#### Total Antioxidant Activity According to Ferric Thiocyanate Method

The basis of this method is the spectrophotometric measurement of the peroxide formed by oxidation in the linoleic acid emulsion at 500 nm. In this study, the inhibition effects of samples on linoleic acid peroxidation of stock solutions were measured by ferric thiocyanate (FTC) method at 25, 50 and 100 µg/mL concentrations [27]. The results were compared with BHA standard inhibition rates (Figure 6 and Figure 7). Total antioxidant activity is generally in direct proportion to increasing absorbance.

The results are calculated according to the equation below

$$\text{Inhibition, \%} = [(A_0 - A_1)/A_0] \times 100$$

$A_0$  = Absorbance value of control;  $A_1$  = Absorbance value of sample

As seen at Figure 6 and Figure 7 the samples of Fe(II), Ni(II), Ru(II), Co(II) and ligand at concentrations of 100 µg/mL inhibited linoleic acid emulsion peroxidation 60.68%, 42.03%, 31.7%, 18.79%, 7.03%, respectively, while BHA inhibited linoleic acid peroxidation 79.05%. Especially the effect of Fe(II) complex and iron reduction effect seen here are compatible with each other however, the effect of Fe(II) complex seen here was not observed in the copper reduction and DPPH radical scavenging results (Figure 7).

Statistical analyzes were performed according to the absorbance results in FRAP and CUPRAC methods and the concentration results obtained in DPPH method. In Table 2, statistical comparisons of the data were performed using Tukey's multiple comparison test of One Way ANOVA and values were showed as mean  $\pm$  standard error (MEAN $\pm$ SEM). In the results, "\*" was used as a symbol for statistical comparison of BHA and samples (ligand and metal complexes), "." was used as a symbol for statistical comparison of TRLX and samples (ligand and metal complexes) and "ns" was used as a symbol of insignificance. According to this, "ns"; for p value > 0.05, "\*/\*"; for p < 0.05, "\*\*/\*"; for p < 0.01, "\*\*\*/\*"; and "\*\*\*/\*"; for p < 0.001 and p < 0.0001 were used [8].

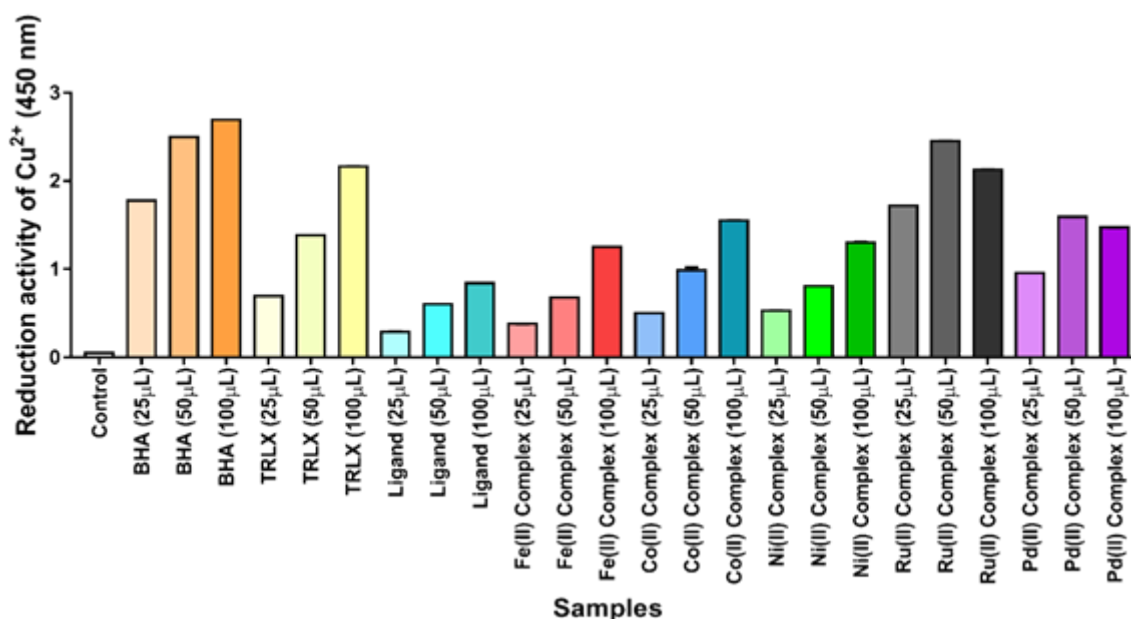


**Figure 5.** Cupric ions ( $\text{Cu}^{2+}$ ) reduction activities of standard antioxidants, ligand and its M(II) complexes using CUPRAC method.

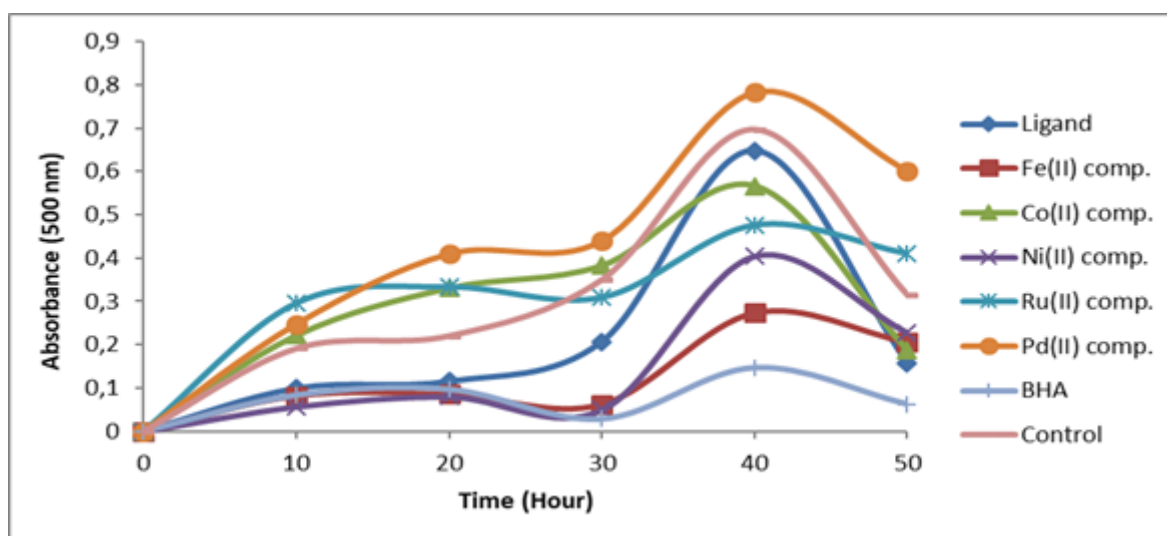


Figure 6. Comparison of total antioxidant activity of ligand and its M(II) complexes with standard antioxidant.

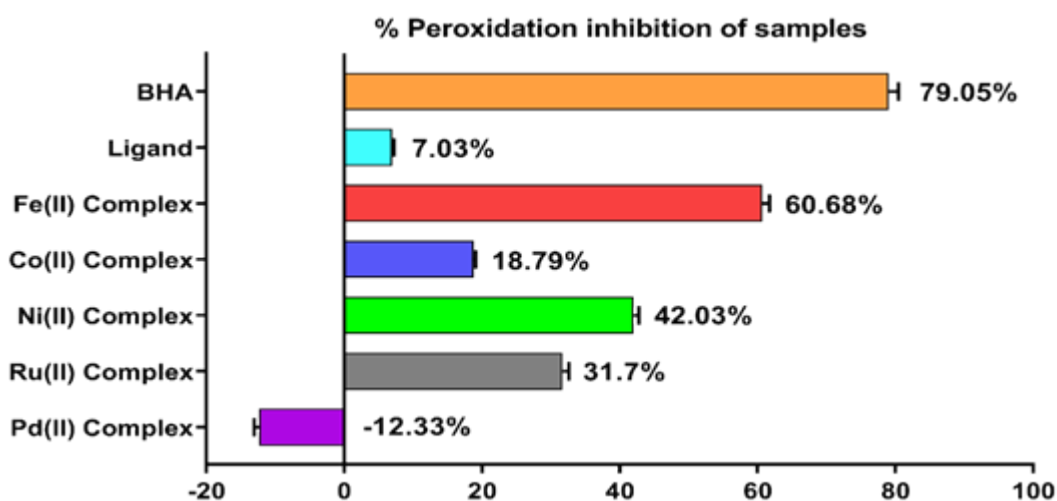


Figure 7. The peroxidation inhibitions in 100 µg/mL concentrations of standard antioxidant, ligand and metal complexes.

## CONCLUSION

A new Schiff base compound and its complexes were synthesized and their structural and spectroscopic properties were determined by FT-IR, UV-Vis,  $^1\text{H}$  and  $^{13}\text{C}$  NMR, microanalyses, magnetic susceptibility, mass spectra and TGA experimental methods. On the basis of electronic spectral data and magnetic susceptibility measurements, suitable geometry was proposed for each complex. The Thermal studies suggested that metal complexes showed several steps thermal degradation. Mass spectrum of the complexes confirmed the proposed structure. Antioxidant properties of the synthesized ligand and complexes were examined according to the four different methods. Considering the outcomes of the study, it was determined that metal complexes showed

better antioxidant activity than ligand. The difference in the activity of metal complexes may be due to the coordination environment and the redox properties.

## ACKNOWLEDGEMENT

We would like to thank to the Muş Alparslan University Scientific Research Foundation for financial support of the project BAP-18-FEF-4902-01. This work was created from the master thesis.

## DECLARATION OF INTEREST

The authors report no conflicts of interest.

Table 2. Statistical analysis results of reduction force of ligand and its M(II) complexes

	Volume, μL	DPPH (C)	DPPH · scavenging activity, %	CUPRAC (ABS <sub>450</sub> )	FRAP (ABS <sub>700</sub> )
BHA*	25	4.999 ± 0.090	74.96	1.779 ± 0.001	0.202 ± 0.002
	50	6.918 ± 0.054	62.89	2.495 ± 0.005	0.278 ± 0.007
	100	4.24 ± 0.084	79.73	2.695 ± 0.002	0.58 ± 0.003
TRLX•	25	6.85 ± 0.007	63.31	0.693 ± 0.003	0.111 ± 0.001
	50	3.571 ± 0.160	83.93	1.385 ± 0.002	0.156 ± 0.001
	100	2.15 ± 0.034	92.87	2.166 ± 0.003	0.227 ± 0.008
Ligand	25	16.29 ± 0.44 ****/••••	3.95	0.292 ± 0.001 ****/••••	0.049 ± 0.001 ns/ns
	50	15.06 ± 0.018 ****/••••	11.68	0.604 ± 0.001 ****/••••	0.050 ± 0.003 ns/ns
	100	16.51 ± 0.089 ****/••••	2.58	0.841 ± 0.001 ****/••••	0.082 ± 0.002 ****/ns
Fe(II) Complex	25	16.52 ± 0.030 ****/••••	2.49	0.378 ± 0.001 ****/••••	0.353 ± 0.296 ns/ns
	50	14.54 ± 0.136 ****/••••	14.95	0.678 ± 0.002 ****/••••	0.081 ± 0 ns/ns
	100	12.23 ± 0.080 ****/••••	29.47	1.251 ± 0.001 ****/••••	0.130 ± 0 ***/ns
Co(II) Complex	25	11.9 ± 0.045 ****/••••	31.53	0.501 ± 0.002 ****/••••	0.054 ± 0.001 ns/ns
	50	15.95 ± 0.060 ****/••••	6.10	0.988 ± 0.034 ****/••••	0.070 ± 0.001 ns/ns
	100	12.27 ± 0.060 ****/••••	29.21	1.554 ± 0.001 ****/••••	0.141 ± 0.001 ***/ns
Ni(II) Complex	25	16.58 ± 0.060 ****/••••	2.10	0.531 ± 0.002 ****/••••	0.052 ± 0.002 ns/ns
	50	15.74 ± 0.060 ****/••••	7.39	0.809 ± 0.001 ****/••••	0.057 ± 0.001 ns/ns
	100	15.51 ± 0.036 ****/••••	8.85	1.304 ± 0.005 ****/••••	0.007 ± 0.002 ****/••••
Ru(II) Complex	25	14.59 ± 0.090 ****/••••	14.65	1.72 ± 0.001 ****/••••	0.060 ± 0.001 ns/••••
	50	11.73 ± 0.054 ****/••••	32.60	2.454 ± 0.001 */••••	0.081 ± 0.002 ns/••••
	100	9.671 ± 0.030 ****/••••	45.58	2.128 ± 0.002 ****/ns	0.114 ± 0.001 ***/••••
Pd(II) Complex	25	8.639 ± 0.035 ****/••••	52.06	0.956 ± 0.001 ****/••••	0.039 ± 0.002 ns/••••
	50	7.861 ± 0.071 ***/••••	56.96	1.593 ± 0.001 ****/••••	0.048 ± 0.001 ns/••••
	100	12.64 ± 0.248 ****/••••	26.93	1.473 ± 0.001 ****/••••	0.057 ± 0.001 ****/••••

## DATA AVAILABILITY STATEMENT

No new data were created in this study. The published publication includes all graphics collected or developed during the study.

## CONFLICT OF INTEREST

The author declared no potential conflicts of interest with respect to the research, authorship, and/or publication of this article.

## ETHICS

There are no ethical issues with the publication of this manuscript.

## REFERENCES

- [1] Rudbari HA, Khorshidifard M, Askari B, Habibi N, Bruno G. New asymmetric Schiff base ligand derived from allyl amine and 2,3-dihydroxybenzaldehyde and its molybdenum(VI) complex: Synthesis, characterization, crystal structures, computational studies and antibacterial activity together with synergistic effect against *Pseudomonas aeruginosa* PTTC 1570. *Polyhedron* 2015;100:180–91. [\[CrossRef\]](#)
- [2] Kachi-Terajima C, Shimoyama T, Ishigami T, Ikeda M, Habata Y. A hemiaminal-ether structure stabilized by lanthanide complexes with an imidazole-based Schiff base ligand. *Dalton Transactions* 2018;47:2638–45. [\[CrossRef\]](#)
- [3] Qian HY, Sun N, Synthesis and crystal structures of manganese(III) complexes derived from bis-Schiff Bases with antibacterial activity. *Transition Metal Chemistry* 2019;44:501–6. [\[CrossRef\]](#)
- [4] Gölcü A, Tümer M, Demirelli H, Wheatley RA. Cd(II) and Cu(II) complexes of polydentate Schiff base ligands: Synthesis, characterization, properties and biological activity. *Inorganica Chimica Acta* 2005;358:1785–97. [\[CrossRef\]](#)
- [5] Xue LW, Han YJ, Zha GQ, Feng YX. Synthesis, structure, and antimicrobial activity of a cadmium(II) complex derived from N,N'-bis(5-chlorosalicylidene) propane-1,3-diamine. *Russian Journal of Coordination Chemistry* 2012;38:24–8. [\[CrossRef\]](#)
- [6] Adiguzel R, Turan N, Buldurun K, Körkoca H. Spectral, thermal and antimicrobial properties of novel mixed ligand-metal complexes derived from saccharinate complexes and azo dye ligand. *International Journal of Pharmacology* 2018;14:9–19. [\[CrossRef\]](#)
- [7] Buldurun K, Turan N, Aras A, Mantarcı A, Turkan F, Bursal E. Spectroscopic and structural characterization, enzyme inhibitions, and antioxidant effects of new Ru(II) and Ni(II) complexes of Schiff base. *Chemistry Biodiversity* 2019;16:e1900243. [\[CrossRef\]](#)
- [8] Turan N, Buldurun K, Alan Y, Savcı A, Çolak N, Mantarcı A. Synthesis, characterization, antioxidant, antimicrobial and DNA binding properties of ruthenium(II), cobalt(II) and nickel(II) complexes of Schiff base containing o-vanillin. *Research on Chemical Intermediates* 2019;45:3525–40. [\[CrossRef\]](#)
- [9] Buldurun K, Turan N, Savcı A, Çolak N. Synthesis, structural characterization and biological activities of metal(II) complexes with Schiff bases derived from 5-bromosalicylaldehyde: Ru(II) complexes transfer hydrogenation. *Journal of Saudi Chemical Society* 2019;23:205–14. [\[CrossRef\]](#)
- [10] Bingöl M, Turan N. Schiff base and metal(II) complexes containing thiophene-3-carboxylate: Synthesis, characterization and antioxidant activities. *Journal of Molecular Structure* 2020;1205:127542. [\[CrossRef\]](#)
- [11] Hassan MU, Chohan ZH, Scozzafava A, Supuran CT. Carbonic anhydrase inhibitors: Schiff's bases of aromatic and heterocyclic sulfonamides and their metal complexes. *Journal of Enzyme Inhibition and Medicinal Chemistry* 2004;19:263–7. [\[CrossRef\]](#)
- [12] Osowole AA, Kempe R, Schobert R. Synthesis, spectral, thermal, in vitro antibacterial and anticancer activities of some metal (II) complexes of 3-(-1-(4-methoxy-6-methyl)-2-pyrimidinylimino) methyl-2-naphthol. *International Research Journal of Pure and Applied Chemistry* 2012;2:105–29. [\[CrossRef\]](#)
- [13] Mohanan K, Murukan B. Complexes of manganese(II), iron(II), cobalt(II), nickel(II), copper(II), and zinc(II) with a bishydrazone. Synthesis and Reactivity in *Inorganic Metal-Organic and Nano-Metal Chemistry* 2005,35:837–44. [\[CrossRef\]](#)
- [14] Nelson SM, Knox CV, McCann M, Drew MGB. Metal-ion-controlled transamination in the synthesis of macrocyclic Schiff base ligands. 1. Reaction of 2,6-diacetylpyridine and dicarbonyl-compounds with 3,6-dioxaoctane-1,8-diamine. *Journal of the Chemical Society Dalton Transactions* 1981;8:1669–77. [\[CrossRef\]](#)
- [15] Kalia SB, Lumba K, Kaushal G, Sharma M. Magnetic and spectral studies on cobalt(II) chelates of a dithiocarbamate derived from isoniazid. *Indian Journal of Chemistry* 2007,46:1233–9. [\[CrossRef\]](#)
- [16] Tanak H, Ađar AA, Büyükğüngör O. Experimental (XRD, FT-IR and UV-Vis) and theoretical modeling studies of schiff base (E)-N'-((5-nitrothiophen-2-yl) methylene)-2-phenoxyaniline. *Spectrochimica Acta Part A* 2014;118:672–82. [\[CrossRef\]](#)
- [17] Mohamed GG. Metal complexes of antibiotic drugs. Studies on diclaxacillin complexes of FeII, FeIII, CoII NiII and CuII, *Spectrochimica Acta Part A* 2001;57:1643–8. [\[CrossRef\]](#)

- [18] Mondal N, Dey DK, Mitra S, Abdul Malik KM. Synthesis and structural characterization of mixed ligand  $\eta^1$ -2-hydroxyacetophenone complexes of cobalt(III), *Polyhedron* 2000;19:2707–11. [\[CrossRef\]](#)
- [19] Kılıç A, Taş E, Kılınç D, Yılmaz İ, Durgun M, Özdemir İ, Yaşar S. The orthopalladation dinuclear [Pd(L1)( $\mu$ -OAc)]<sub>2</sub>, [Pd(L2)( $\mu$ -OAc)]<sub>2</sub> and mononuclear [Pd(L3)]<sub>2</sub> complexes with [N, C, O] or [N, O] containing ligands: Synthesis, spectral characterization, electrochemistry and catalytic properties. *Journal of Organometallic Chemistry* 2010;695:697–706. [\[CrossRef\]](#)
- [20] Kavitha P, Laxma Reddy K. Pd(II) complexes bearing chromone based Schiff bases: Synthesis, characterization and biological activity studies, *Arabian Journal of Chemistry* 2016;9:640–8. [\[CrossRef\]](#)
- [21] Ceyhan G, Köse M, McKee V, Uruş S, Gölcü A, Tümer M. Tetradentate Schiff base ligands and their complexes: Synthesis, structural characterization, thermal, electrochemical and alkane oxidation, *Spectrochimica Acta Part A* 2012;95:382–98. [\[CrossRef\]](#)
- [22] Yu SY, Yoo SJ, Yang L, Zapata C, Srinivasan Hay BA, Baker NE. A pathway of signals regulating effect or and initiator caspases in the developing *Drosophila* eye. *Development* 2002;129:3269–78. [\[CrossRef\]](#)
- [23] Awika JM, Rooney L W, Wu X, Prior RL, Cisneros-Zevallos L. Screening methods to measure antioxidant activity of sorghum (sorghum bicolor) and sorghum products, *Journal of Agricultural and Food Chemistry* 2003;51:6657–62. [\[CrossRef\]](#)
- [24] Gülçin İ. Antioxidant activity of caffeic acid (3,4-dihydroxycinnamic acid), *Toxicology* 2006;217:213–220. [\[CrossRef\]](#)
- [25] Silinsin M, Bursal E. UHPLC-MS/MS phenolic profiling and in vitro antioxidant activities of *Inula graveolens* (L.) Desf. *Natural Product Research* 2016;32:1467–71. [\[CrossRef\]](#)
- [26] Çekiç SD, Sözgen Başkan K, Tütem E, Apak R. Modified cupric reducing antioxidant capacity (CUPRAC) assay for measuring the antioxidant capacities of thiol-containing proteins in admixture with polyphenols. *Talanta* 2009;79:344–51. [\[CrossRef\]](#)
- [27] Gülçin İ. Antioxidant and antiradical activities of L-Carnitine. *Life Sciences* 2006;78:803–11. [\[CrossRef\]](#)